Maximum entropy principle underlies wiring length distribution in brain networks

Yuru Song[1], et al

1 School of the Gifted Young, University of Science and Technology of China, Hefei, Anhui, China

Abstract

A brain network in general comprises a substantial amount of short range connections with an admixture of long range connections. Despite this common feature, the portion of long range connections between neurons or brain areas are observed to be quantitatively dissimilar for different species. It is hypothesized that wiring length is constrained by the spatial embedding of brain networks, yet fundamental principles that underlie the wiring length distribution remain to be elucidated. By quantifying the structural diversity of a brain network using the measure of Shannon's entropy, here we show that the wiring length distributions across multiple species——including *C. elegans*, mouse, macaque, *Drosophila*, and human——share the feature of large entropy. Furthermore, these distributions can be well predicted by maximizing the entropy of wiring length under the constraints of limited wiring material and the spatial locations of neurons or brain areas. In addition, by taking into account stochastic axonal growth, we propose a developmental process capable of reproducing wiring length distributions of the five species as measured in experiments, thereby implementing the maximum entropy principle in a biologically plausible manner. We further develop a generative model incorporating the maximum entropy principle, and show that, for the five species, the network reconstructed by the generative model exhibits higher similarity to the real network compared with those reconstructed by alternative models without accounting

for network entropy. Our work suggests that the connectivity of brain networks evolves to be structurally diversified to support its complex functions such as efficient inter-areal communication, thus provides a potential organizational principle of spatially embedded brain networks.

Introduction

The dynamics of a brain network is substantially affected by its comprehensive connections. For instance, it has been shown that the functional connectivity recovered from resting-state cortical dynamics largely overlaps with the structural connectivity [1, 2]. In addition, cortical wave dynamics are often observed in the brain [3, 4]. Theoretical studies indicate that these waves originate preferably from hub areas in the network [5], and the emergence of the waves is influenced by the topology and connection distance of the network [6]. The structural topology of the brain also highly correlates with the spatial gradients of specific brain functions [7]. Consequently, pathological perturbations to the brain structure will result in various brain disorders, as reviewed in Ref. [8]. For instance, in contrast to healthy controls, schizophrenia patients have a reduced hierarchical structure and an increased connection distance in their anatomically connected network of multi-modal cortex [9]. It is hypothesized that childhood-onset schizophrenia is induced by the overpruning of short distance connections during the developmental stage [10].

To quantitatively characterize the structure of brain networks, tools from graph theory and network science have been introduced into the neuroscience field [11, 12]. Following the conventions of network terminology, neurons or brain regions are often described as nodes and the connections between them are described as edges. Subsequently, network measurements including node degree distributions, clustering coefficients, path lengths, assortativity, and modularity have been calculated based on

experimental measurements. It has been found that brain networks exhibit features of complex networks with highly connected hubs [13, 14] and modularity [14–16]. These network features are believed to facilitate functional integration and segregation of distinct brain regions [17–19]. In addition, brain networks have been identified with the small-world property characterized by small shortest path lengths and high clustering coefficients [20–22], which presumably maximizes the complexity of brain functions meanwhile minimizing wiring costs [21].

In addition to the aforementioned rich topological features, brain networks also possess the geometrical feature of spatial embedding [23]. This imposes constraints on the network structure [24, 25]. In fact, the gradients of growth factors across space largely determines the network formation during brain development [14]. As a consequence, neurons with similar functions tend to have more similar connection profiles than neurons with less similar functions [26, 27]. In addition, because brain networks are confined in a limited space, the number of neurons as well as the distance and cross-sectional diameter of axonal projections are substantially constrained by space [14]. Furthermore, the cost of establishing and maintaining axonal wiring connections increases with the wiring length of inter-neuronal connections [28]. To minimize wiring cost, a large number of connections in brain networks are observed to be local short connections [29, 30].

As a basic structural characteristic of brain networks, the distribution of wiring length has been measured in recent experiments. In general, the wiring length distribution is observed to peak at a short distance level and tail at a long distance level across multiple species [31, 32]. This fact indicates that brain networks comprise a substantial amount of short range connections with an admixture of long range connections. The long range connections increase the wiring cost, and in return for this, they presumably bring important functional benefits such as supporting efficient

communication [33] and facilitating functional diversity [32]. To further quantify the portion of long range connections, the shape of wiring length distribution has been statistically analyzed across species. In particular, the wiring probability as a function of distance between neurons in the neural network of *C. elegans* is best fitted by a power law distribution, and that in the neuronal network of rat visual cortex is best fitted by a Gaussian distribution [31]. In the inter-area network of macaque, the dependence of wiring probability on distance has been reported as gamma [31] and exponentially distributed [34] in two independent studies, respectively. Using scaling-theory, power-law distribution is theoretically proved to be the optimal solution of wiring length distribution [35].

Based on experimental observations, computational models have been developed to capture the distribution of wiring length. In particular, generative models have been proposed to well fit the wiring length distributions of macaque and human brain networks, respectively [34, 36, 37]. Yet these models often contain free parameters to be determined by fitting the network statistics. Accordingly, they are incapable of predicting the wiring length distribution without specifying the optimal parameter sets, thus impeding the understanding of the principle underlying the wiring length distribution. Alternatively, optimization models suggest that the wiring length distribution of the macaque brain network is optimally determined from the trade off between wiring cost and functional efficiency [38]. However, in contrast to the definition of wiring cost [28, 39], the definition of functional efficiency sofar remains to be ambiguous. Therefore, the functional efficiency referred to as the short path length in the optimization model [38] is arguable [32, 36].

As a further step to understand the organizational principle of brain networks, the following questions need to be addressed: (1) What is the common feature of the wiring length distributions across different species, if any? (2) Is there a fundamental principle

underlying the wiring length distribution of a brain network? (3) How does the experimentally observed wiring length distribution emerge during network formation? (4) Are the experimentally observed wiring length distribution optimally designed for any brain function?

In this work, by quantifying the structural diversity of a brain network using the measure of Shannon's entropy [38, 40, 41], we show that the wiring length distributions across multiple species——including *C. elegans*, mouse, macaque, *Drosophila*, and human——share the common feature of large entropy. Furthermore, these distributions can be well predicted by maximizing the entropy of wiring length under the constraints of (1) the spatial locations of neurons or brain areas and (2) the limited material resource described by average wiring length. This predictive framework is parameter-free as the information of the two constraints is explicitly read out from experimental observations. In addition, by considering stochastic axonal growth [31, 42], we propose a potential process of network development to reproduce the wiring length distributions for multiple species as observed in experiments, thereby implementing the maximum entropy principle in a biologically plausible manner. We further develop a generative model incorporating the maximum entropy principle, and show that, for the five species, the network reconstructed by the generative model is more similar to the real network compared with those reconstructed by alternative models without accounting for network entropy. Finally, we show that the functional implications of structural diversity, and the predictability of the maximum entropy principle for other transport networks including airport in the United States, California road, and Shanghai subway are discussed.

Materials and methods

Data source

We analyze the network structure of *C. elegans*, *Drosophila*, mouse, macaque, and human brain. The connections are measured between neurons for *C. elegans*, while the connections are measured between brain areas for other species. In our analysis, we focus on the wiring length distribution of a network. Accordingly, we use the binary information of the network connectivity, i.e., the information of whether two areas are connected or not, although the network *per se* is directed and weighted. The data we use for analysis are obtained from the sites described below.

C elegans. Two datasets for *C elegans* are accessible online: `https://www.wormatlas.org` and `https://www.dynamic-connectome.org`. Both are based on the electron micrographs published in [43], with new reconstructions of synapse. The first dataset is provided and analyzed in [44–46], incorporating new updates in other works [47, 48]. It covers 280 neurons, 6393 chemical synapses, 890 electrical junctions, and 1410 neuromuscular junctions. In addition, the positions of soma projected onto the anterior-posterior axis of the worm body are provided. The second dataset is published by [49, 50]. It includes 277 neurons and 2105 synapses, as well as the two-dimensional spatial positions of the neurons. The connectivity information of the 277 neurons doesn't fully overlap between these two datasets. We keep those synapses the two datasets have in common and also combine the synapses they own seperately, which yields 4758 synapses in our dataset. We use the two dimensional geometric information from the second dataset. We divide a local neuronal network within the C elegans neural network based on the spatial positions of neuron (see Supplementary Fig S1). This local network contains 169 spatially frontal neurons and 1331 connections between them.

Drosophila. The network connectivity for Drosophila was reconstructed from the

FlyCircuit 1.1 database (`http://www.flycircuit.tw`). It is a repository of images of 12,995 projections in the female Drosophila brain. Neurons were labeled with green fluorescent protein (GFP) using genetic mosaic analysis, and were delineated from whole brain images and co-registered to a female template brain using a rigid linear transform. Individual neurons were partitioned into 49 local areas with distinct morphological and functional characteristics. Areas were defined so as to contain their own population of local interneurons whose fibers were limited to that area.

Mouse. The network connectivity for mouse was reconstructed based on tract-tracing data from the Allen Institute Mouse Brain Connectivity Atlas (`http://connectivity.brain-map.org`). Anterograde recombinant adeno-associated viral tracer was injected into target areas in the right hemisphere of mouse brains. Viral tracer projection patterns were reconstructed three weeks after tracer injection. Reconstructions were then smoothed and aligned to a common coordinate space of the Allen Reference Atlas. Network areas were defined according to a custom parcellation based on the Allen Developing Mouse Brain Atlas. This parcellation contains 65 areas in each hemisphere, 9 of which were removed because they were not involved in any tract-tracing experiment. The resulting network contained 112 areas and 6542 connections.

Macaque. The online CoCoMac database (`http://cocomac.g-node.org/main/index.php`) covers connectivity data across literatures on tract-tracing experiments in macaque brain [51–54]. Later analysis of the database provides a direct repository of spatial positions of 95 cortical areas and 2390 connections between areas, which are available on `https://www.dynamic-connectome.org` [49]. In more recent work [55], the dataset is improved and expanded to 103 cortical nodes and 2518 connections using a more detailed parcellation of the motor regions. The updated dataset is also discussed in [38].

Human. The human brain network includes 128 cortical areas and 4736 connections. It is reconstructed from diffusion weighted MRI, based on deterministic tractography algorithms. The data represents the composites of 30 human subjects. The data is provided by authors in [32].

Generative models

We propose a generative model to demonstrate that the maximum entropy principle involves in determining the brain network structure, in contrast to alternative models without considering network entropy.

The generative model is modified from Ref. [56] and is described as follows. In the model, the spatial locations of brain areas and their degree sequence are given from the real brain network we attempt to reconstruct, and the Euclidian distance between each pair of areas is calculated. To predict the network connectivity and statistics, we initialize the network by disconnecting all the areas, i.e., there is no connection in the initial network thus each area has a zero degree. We then create a candidate list to include all the areas whose current degree is less than the target degree given by the degree sequence, and we put all the areas' ID into the candidate list initially. We next introduce an objective function $F = H - \lambda * \bar{d}$ to help select a pair of areas and connect them at each connection generating step, where H is the entropy of the network defined as $H = -\sum_{i=1}^{k} p_i \log(p_i)$ and p_i is the probability of finding a connection with its length falling into the range $[d_i, d_i + 1)$ in the current network, $\bar{d}$ is the material cost or the average wiring length of the current network, and λ is a free parameter that scales the relative importance between network entropy and material cost. The value of λ is chosen as 113 for *C elegans* global network, 339 for *C elegans* local network, 0.121 for *Drosophila* network, 0.791 for mouse network, 0.187 for macaque network, and 0.494 for human network, based on the best performance of network reconstruction of the model. In each step of connection generation, we utilize the greedy searching strategy: (1) For

each area V_i in the candidate list, hypothetically connect it to another area V_j in the candidate list whose current degree has the largest difference from its target degree. (2) For each pair of V_i and V_j, compute the objective function F after adding the hypothetical connection between V_i and V_j. (3) Select the pair of V_i and V_j to connect which corresponds to the largest F. (4) Update the current degree of V_i and V_j, and update the candidate list if the degree of V_i or V_j reaches its target number. (5) Repeat the above steps until the candidate list becomes empty.

Note that the objective function F in the generative model takes the Lagrange Multiplier form of the optimization problem (Eq. 1) constrained by the material cost (Eq. 3), and the generative model naturally satisfies the constraints of probability normalization (Eq. 2) and space (Eq. 4). Therefore, the generative model locally optimizes network entropy constrained by material cost and space in each step. We refer this model to as the MaxEnt-MinCost model. The MaxEnt-MinCost model further provides more information than the solution of the optimization problem (Eq. 1-4), i.e., the additional information of network connectivity and statistical properties beyond the wiring length distribution. Therefore, the MaxEnt-MinCost model allows us to investigate the role of the maximum entropy principle in determining network structure and property. To substantiate the unique role of the maximum entropy principle in network structure, we further develop four alternative generative models for comparison as described below. The first two models are slightly modified from the aforementioned generative model by replacing the objective function $F = H - \lambda * \bar{d}$ with $F = H$ and $F = -\bar{d}$ respectively, in order to isolate the impact of network entropy and material cost on network structure respectively. These two models are referred to as the MaxEnt model and the MinCost model respectively. In the third model, we randomly choose a pair of areas to connect under the constraint of degree sequence in each step rather than based on F, thus removing the impacts of both entropy and material cost on network

structure. This model is referred to as the fixed-degree random model. The forth model further removes the constraint of degree sequence. The network is reconstructed by randomly choosing a pair of areas to connect in each step until the number of connections reaches that of the real brain network measured in experiment. This model is referred to as the random-degree random model.

Results

Maximum entropy principle predicts the wiring length distributions

The brain network in general consists of both short-range and long-range connections. It is evident that short-range connections can substantially save material cost. In contrast, long-range connections utilizes more material, which presumably benefits certain brain functions. However, the functional role of long-range connections remains to be fully elucidated, which impedes one to understand the spatial organization principle of the brain network. As the definition of network function remains arguable, here we investigate the organization principle from a different angle. Rather than exploring the functional benefits of network structure, we explore the question of what is the universal structural characteristic that brain networks evolve to possess, as whatever functional benefits are supported by the network structure. We are particularly interested in the wiring length distribution of brain networks, which reveals the portion of short and long range connections that the brain invests resource to establish.

To address this question, we first analyze brain networks of four species —— *Drosophila*, mouse, macaque, and human. The connections in these four networks are measured between brain areas (see Material and Methods for details). In addition, the wiring length d between two brain areas are measured by using the Euclidian distance,

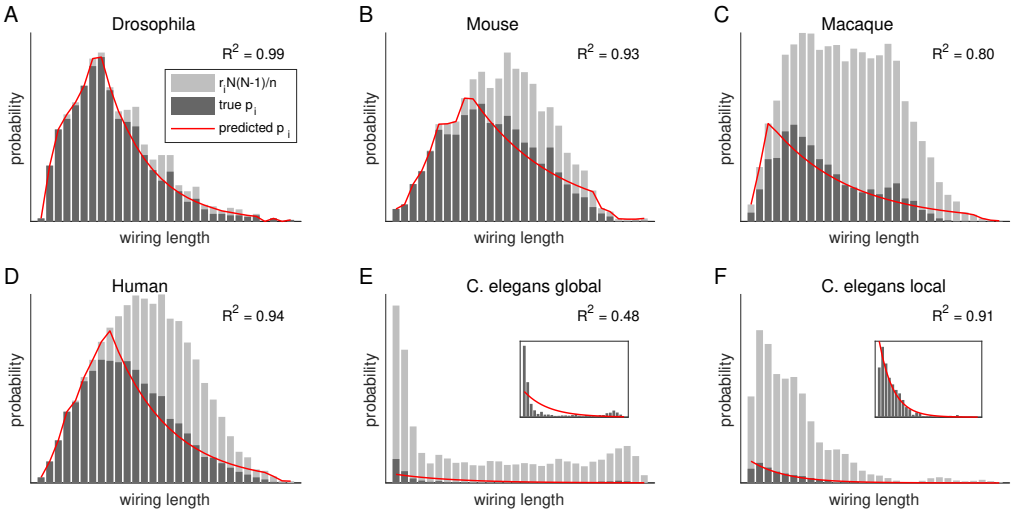

Fig 1. Wiring length distributions of multiple species and their predictions by the maximum entropy principle. (A)-(D) are for networks of Drosophila, mouse, macaque, human, respectively. (E) and (F) are for the global and local networks of C. elagans, respectively. The insets of (E) and (F) are zooming in. In each panel, dark gray bars are the distribution measured from experiments. Silver bars are the reference distribution defined in the main text. Solid line is the distribution predicted by the maximum entropy principle (Eqs. 1-4). R^2 is calculated to evaluate the performance of the prediction.

and all the wiring lengths are partitioned into even bins $[d_i, d_{i+1})$, $i = 1, 2, ..., k$ to calculate the wiring length distribution $p_i = Pr(d \in [d_i, d_{i+1}))$. For the purpose of result demonstration, the number of bins is set to be $k = 30$ for processing data obtained from different species, yet the results shown below are insensitive to the choice of bin number. As shown in Fig. 1, despite the fact that all the distributions of wiring length are unimodal, the shapes of these distributions are dissimilar. For instance, the wiring length distribution for macaque is heavily skewed, while that for human is nearly symmetric. The dissimilarity among the wiring length distributions for different species is caused by at least two factors, i.e., the geometric locations of brain areas as the constraint of space, and the total wiring length as the constraint of material cost.

To demonstrate the spatial constraints on a brain network, we first define the reference distribution as $\frac{N}{M} \cdot q_i$, where M is the number of connections in the real brain network, N is the number of connections in a corresponding fully connected brain

network consisting of the same brain areas as the real brain network, and q_i is the wiring length distribution of the fully connected brain network. As shown in Fig. 1, the wiring length distribution p_i is always under the reference distribution for all networks, i.e., $p_i \leq \frac{N}{M} \cdot q_i$. This can be explained by the fact that the number of connections with wiring length falling into the bin $[d_i, d_{i+1})$ shall be no larger than the number of all available connections with wiring length falling into the same bin, i.e., $p_i \cdot M \leq q_i \cdot N$. In this sense, p_i is constrained by the spatial locations of brain areas. In addition, for all the four networks, we note that the rising part of the wiring length distribution p_i nearly overlaps with the rising part of the reference distribution. Their overlap indicates that the brain network exploits almost all the short-range connections that are available to form. This observation supports the hypothesis that the brain network tends to form short-range connections in order to save material cost. Furthermore, as shown in Fig. 1, for all the four networks, the decay part of the wiring length distribution exhibits a substantial difference from their reference distribution. This observation suggests that the brain network choose to form only a portion of long-range connections instead of all of the available ones, which presumably results from the constraint of wiring resource.

Note that the constraints of space and material are not sufficient to determine the wiring length distribution. In fact, under the two constraints, it remains feasible for the brain network to form additional long-range connections in compensation for removing short-range connections, and *vice versa*. Therefore, revealing the principle underlying the wiring length distribution is still an open question. It is hypothesized that the network structure is optimized for information processing functionally. However, the definition of functional efficiency of the brain remains ambiguous. Because the diverse function of the brain shall be supported by the network structure, we hypothesize that the network structure is optimally diversified though evolution.

Driven by this hypothesis, we introduce the measure of Shannon's entropy to

quantify the diversity of the network structure. The entropy of a network is defined as $H = -\sum_{i=1}^{k} p_i \log(p_i)$. By calculating the entropy of the four brain networks, we find that all of them show entropy values as 4.0126 ± 0.3436. For reference, we rewire each of the four networks such that every brain area connects to an equal number of its nearest neighbouring areas while the total number of connections is unchanged. We subsequently calculate the entropy of these "spatially regular" networks as 3.9364 ± 0.4519, which is significantly smaller than the entropy of the real brain networks. The large entropy of these brain networks across different species attributes to their broad wiring length distributions, which indicates the large structural diversity of these networks.

We next investigate the question of whether entropy maximization is sufficient to determine the wiring length distribution in addition to the constraints of space and material cost. We find that the wiring length distribution of all the four brain networks can be well predicted by the optimal solution of the following optimization problem,

$$\text{maximize} \quad -\sum_{i=1}^{k} p_i \log(p_i) \tag{1}$$

$$\text{subject to} \quad \sum_{i=1}^{k} p_i = 1 \tag{2}$$

$$\sum_{i=1}^{k} p_i \cdot d_i \leq \bar{d} \tag{3}$$

$$p_i \leq \frac{N}{M} q_i \quad \text{for} \quad i = 1, 2, ..., k \tag{4}$$

where Eq. 2 (probability constraint) is the normalization condition for probability p_i; Eq. 3 (material constraint) requires the average wiring length to be no larger than an upper bound $\bar{d}$, which is measured as the average material cost in each brain network we aim to predict; Eq. 3 (space constraint) requires that the number of connections

with wiring length in the range $[d_i, d_{i+1})$ cannot exceed the number of all available connections with wiring length in the same range.

We use CVX, a platform for specifying and solving convex programs [57, 58], to find the global optimal solution of the convex optimization problem (Eqs. 1-4) for each of the four brain networks, i.e., *Drosophila*, mouse, macaque, human brain. As shown in Fig. 1A-D, the optimal solutions well overlap with the experimentally observed wiring length distributions for all the four brain networks. Further, R^2 is calculated to quantify the performance of the predictions—$R^2 = 0.99$ for *Drosophila* network, $R^2 = 0.93$ for mouse network, $R^2 = 0.80$ for macaque network, and $R^2 = 0.94$ for human network. In addition to analyzing the four brain networks with connections measured between brain regions, we have also analyzed the *C. elegans* network in which connections are measured between neurons. As shown in Fig. 1E, the prediction from the maximum entropy principle fits the observed wiring length distribution moderately well with $R^2 = 0.48$. However, the performance of the prediction can be substantially improved in Fig. 1F with $R^2 = 0.91$ by considering a local network consisting of 60% neurons of the whole population that are located in the frontal area of the *C. elegans*.

We point out that the constraint of material cost in the optimization problem (Eqs. 1-4) is loosely set with an upper bound, which allows a network to use less material than the real one measured in experiment. This constraint together with the other two constraints ensure a large feasible region of the optimization problem (Eqs. 1-4), i.e., there are a large number of possible solutions that satisfy the constraints. However, the objective function of entropy maximization picks out only one solution that is consistent with the wiring length distribution observed in the real brain network, indicating that entropy maximization can be a potential principle of brain network organization.

Biological implementation of the maximum entropy principle

We next investigate biologically plausible implementation of the maximum entropy principle during the stage of network wiring formation. It has been found that neural wiring is determined by multiple factors, including gene expression [26, 59], gradients of growth factors [14], randomness of axonal growth [31, 42, 60] and others. Here we hypothesize that stochastic axonal growth may play an important role in implementing the maximum entropy principle, as the concept of entropy in general characterizes the degree of randomness of a physical quantity.

Fig. 2A-C illustrates the process of network formation by stochastic axonal growth. In the model, the locations of all brain areas are embedded in the geometric space, and the distance between each pair of brain areas is set to be identical to that measured in experiment. Initially all brain areas are disconnected. A bunch of axons start to grow out with a constant speed from each area towards random directions. The growth of an axon terminates once the axon reaches the vicinity of another area if that area has not been fully occupied. After sufficiently long simulation time, axons that fail to connect two areas will be pruned. To avoid the emergence of super rich hubs with unrealistically large number of degrees, each area is set to have a limited number of axons it can receive. In our numerical simulations, this bound for each area is set to equal the actual degree of the area. In addition, the radius of the "touching field" is chosen such that the total number of connections approximately equals that of the real brain network. Additional stochasticity is introduced by setting a fixed probability of allowing new synapses among candidates. Such randomness enlarges the chance of connecting distant areas. The exact values of these biological parameters, including the number of outgrowing axons, the speed of axonal growth speed, the radius of the "touching field", and the probability of forming new connection, vary for the 6 neural networks and are listed in the Supplementary Table 1. As shown in Fig. 2D-I, the random growth model

well reproduces the wiring length distribution for all the brain networks across the five species, although the reproducing of the wiring length distribution for the *C. elegans* global network is moderately well. This result indicates that random axon growth may serve as a crucial factor that implements the maximum entropy principle.

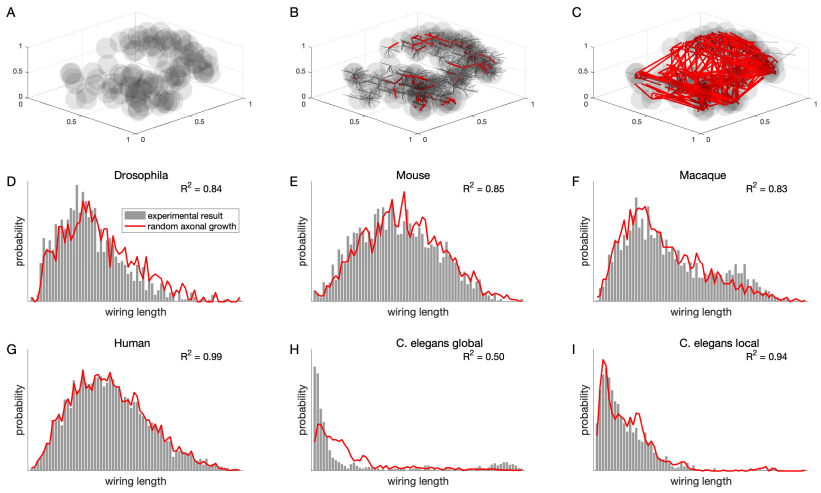

Fig 2. Random axonal growth process reproduces the wiring length distributions of multiple species. (A)-(C) Schematic illustration of the random growth process. (A) The initial state of a network with all areas disconnected. The locations of all the areas are based on experimental measurement. Gray spheres are the "touching field" of each area. (B) The random growth stage of the network. A bunch of axons start to grow out with a constant speed from each area towards random directions. Connections are formed (red lines) when growing axons (black lines) fall into the touching field of an area. (C) The pruning state of the network. Networks are formed by pruning axons that fail to connect two areas. (D)-(G) are the wiring length distributions for brain networks of Drosophila, mouse, macaque, human, respectively. (H) and (I) are for the global and local networks of *C. elagans*, respectively. The silver bars are from experimental measurement, and the black curves are from the simulations of random axonal growth.

Maximum entropy principle contributes to additional network properties

We further address the question of whether the principle of maximum entropy contributes to additional properties of network structure beyond the wiring length distribution. For instance, network connectivity, clustering coefficient, and modular

structure. The investigation of these network properties requires the recovery of network connections, which cannot be directly obtained from the wiring length distribution by solving the optimization problem (Eqs. 1-4).

To overcome this difficulty, we propose a generative model with the maximum entropy principle incorporated (see model details in Materials and Methods). In brief, in the generative model, the degree sequence is initially specified based on experimental measurements. And the model maximizes the quantity $F = H - \lambda * \bar{d}$ at each connection generating step, where H is the entropy of the network, $\bar{d}$ is the material cost or the average wiring length of the network, and λ is a parameter that scales the relative importance between network entropy and material cost. We refer this model to as the MaxEnt-MinCost model, because the maximization of F allows the model to reconstruct the network connectivity that optimally balances the maximization of network entropy and the minimization of material cost. To substantiate the unique role of the maximum entropy principle on network structure, we further develop four alternative generative models for comparison. The first two models are slightly modified from the MaxEnt-MinCost model by replacing the quantity $F = H - \lambda * \bar{d}$ with $F = H$ and $F = -\bar{d}$ respectively, which isolates the impact of network entropy and material cost on network structure respectively. These two models are referred to as the MaxEnt model and the MinCost model, respectively. In the third model, we randomly connect a pair of areas only under the constraint of degree sequence in each step rather than optimizing F, thus removing the influence of both entropy and material cost on network structure. The model is referred to as fixed-degree random model. The forth model further removes the constraint of degree sequence, thus is referred to as rand-degree random model.

We first assess the performance of the generative models on the recovery of the network connectivity, which is evaluated by the recovery rate defined as the ratio of the

number of successfully recovered connections by a generative model to the total number of existing connections in the real network. As shown in Fig. 3A, across all the five species, the recovery rate of the MaxEnt-MinCost model is systematically higher compared with the other four generative models. The result demonstrates that network connectivity depends on the maximization of network entropy, the minimization of material cost, and the constraint of degree sequence as considered in the MaxEnt-MinCost model. The recovery rate drops by either removing the condition of entropy maximization (the MinCost model) or material cost minimization (the MaxEnt model) from the MaxEnt-MinCost model. Therefore, it is the balance of maximizing network entropy and minimizing material cost that plays an important role in determining network structure. The decrease of recovery rate from the MaxEnt-MinCost model to the MaxEnt model is about 11.58% $\pm$7.90% (mean $\pm$ standard deviation for six networks across five species), which is more significant than that from the MaxEnt-MinCost model to the MinCost model about by 3.74% $\pm$ 2.07%, suggesting that the removal of the material cost constraint has a larger effect on network structure than the removal of the network entropy constraint. In other words, the minimization of material cost influences more on network structure than the maximization of network entropy. By further removing both the constraints of network entropy and material cost, the recovery rate further decays from the MaxEnt-MinCost model to the fixed-degree random model by 13.3% $\pm$ 9.17% for all the five species. And the recovery rate from the random-degree random model is lowest when removing the last constraint of fixed-degree — with a drop of recovery rate by 15.35% $\pm$ 11.26%, indicating that degree sequence is informative for the reconstruction of network connectivity.

As shown in Fig. 3A, the recovery rate from all the generative models for *Drosophila* is highest as above 90%, which mainly attributes to its dense network connections. In contrast, the recovery rate from all the models for *C. elegans* is lowest as below 30%

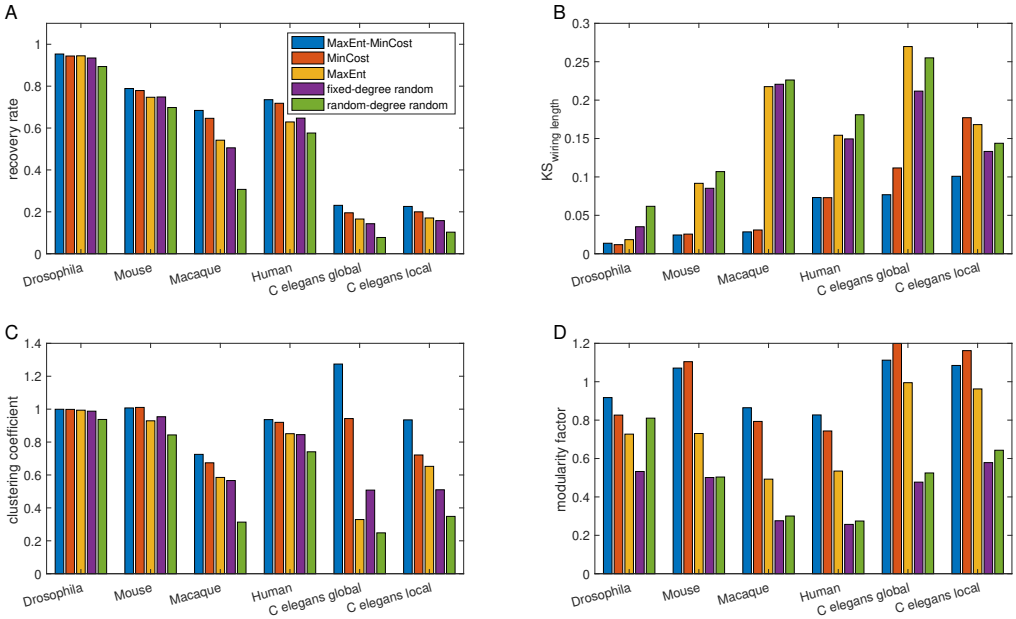

Fig 3. Performance of the generative models on the prediction of network properties for the five species. (A) recovery rate. (B) Kolmogorov–Smirnov statistic of the wiring length distribution measured in experiment and that recovered by the generative models. (C) Network clustering coefficient. (D) Network modularity factor. (A)-(D) share the same legend in (A).

which mainly attributes to its sparse network connections. At present, an accurate reconstruction of network connectivity remains a challenging task. Here the imperfect reconstruction for networks of the five species suggests the existence of other important factors that have not been taken into account by these generative models. However, the results sufficiently demonstrate the contribution of network entropy to network connectivity, although less substantial compared with that of material cost and degree sequence based on the improvement of the recovery rate of network connectivity.

We further show that maximizing network entropy in the generative models also improves the recovery of network in its statistical aspects including wiring length distribution, clustering coefficient, and modularity factor. In Fig. 3B, we evaluate the performance of the generative models on recovering wiring length distribution using the Kolmogorov–Smirnov(K-S) statistic [61] [62]. By its definition, given a measured wiring length distribution and its prediction, the smaller the K-S statistic value is, the closer

the predicted wiring length distribution is to the real distribution. Therefore, a smaller value of the K-S statistic indicates a better prediction from a generative model. As shown in Fig. 3B, among the five generative models, the MaxEnt-MinCost model best predicts the wiring length distribution of the brain networks from the five species, and the performance significantly drops by removing the constraint of either entropy maximization alone (the MinCost model), or the balance between entropy maximization and material cost minimization (the fixed-degree random model), consistent with the previous result that the maximum entropy principle helps predict the wiring length distributions (Eqs. 1-4). Similar hierarchy of model performance on the recovery of clustering coefficient [20] and modularity factor [63] are shown in Fig. 3C and Fig. 3D respectively. The MaxEnt-MinCost model and the MaxEnt model that account for network entropy maximization in general outperform the fixed-degree random model and the random-degree random model without maximizing network entropy, particularly for the recovery of network modular structure. The successful recovery of the feature of network modularity by the MaxEnt-MinCost model is further demonstrated in Fig. 4, which clearly shows the effectiveness of the MaxEnt-MinCost model in contrast to the fixed-degree random model and the random-degree random model.

Functional implications of the maximum entropy principle

It is generally believed that the structure of a brain network supports its functional efficiency. We have shown that the structure of brain networks across various species share the common feature of large entropy or structural diversity, however, the functional benefit of structural diversity remains unclear. Previous works suggest that the efficiency of brain information processing can be possibly evaluated by the communication speed, i.e., the time it takes a neuronal signal to transmit from one area to another area [14]. One way to estimate the communication speed is to use the

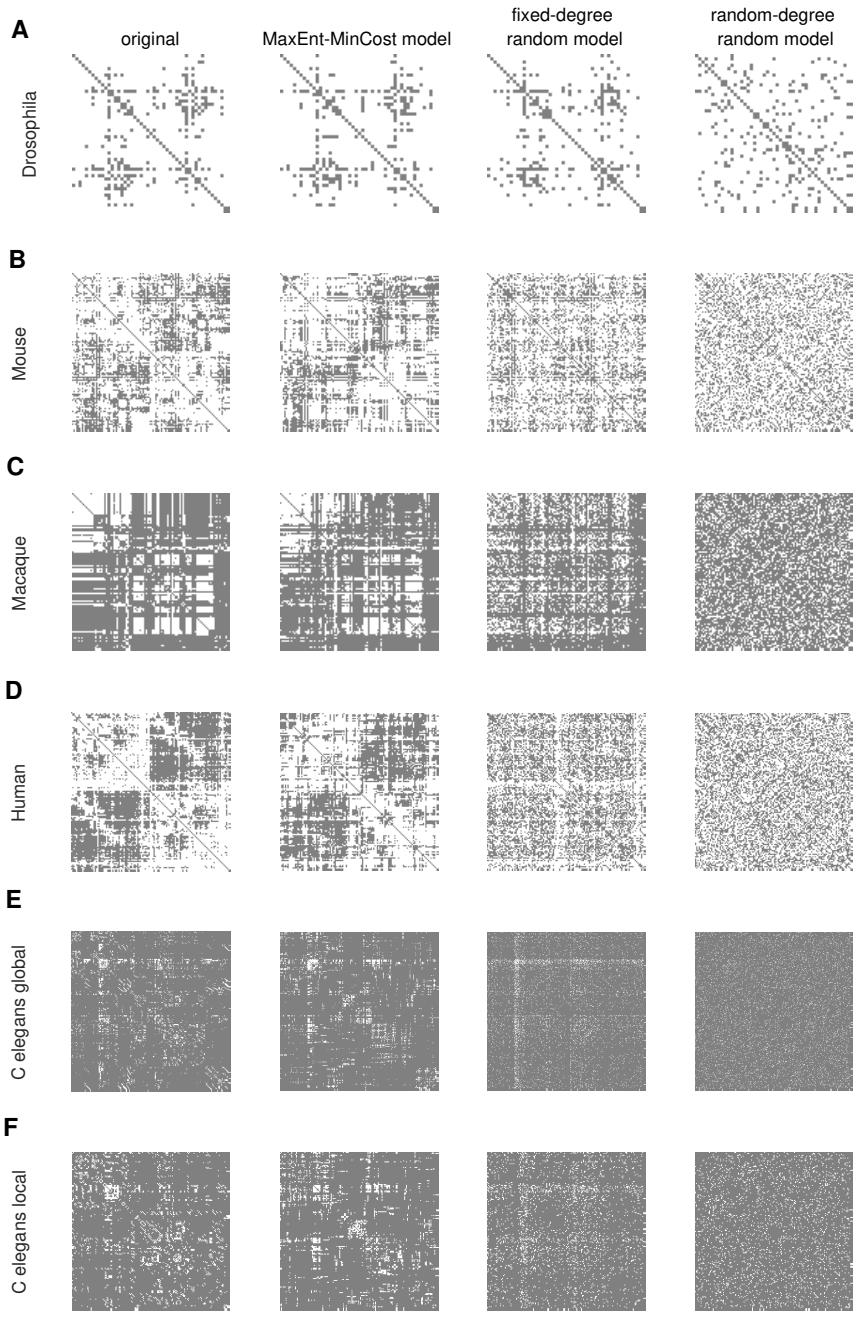

Fig 4. Reconstruction of network connectivity from the generative models. (A) *Drosophila* network. (B) Mouse network. (C) Macaque network. (D) Human network. (E) Global network of *C. elegans*. (F) Local network of *C. elegans*. In each panel, the connectivity matrices recovered from the MaxEnt-MinCost model, the fixed-degree random model, the random-degree random model are compared with the connectivity matrix of the real brain network. The MaxEnt-MinCost model well recovers the modular structure of the real network, while other models fail to recover it.

average shortest path (ASP) of the network [20]. By using mathematical analysis, we will first show that large structural diversity indeed corresponds to small ASP in an idealized brain network in which areas are evenly spaced in a ring. In addition, we will further show that the strong correlation between structural diversity and ASP can also be observed in four out of the six real brain networks measured in experiments. Therefore, a possible functional implication of structural diversity is to benefit information transmission in brain networks.

We first build an idealized brain network based on Ref. [64], in which ASP has been analytically calculated. As shown in Fig. 5A , in the idealized network, we consider L brain areas located evenly in a ring lattice. Each area connects to its nearest $2k$ neighboring areas. In addition, a certain number of long-range shortcuts are added to the network to connect pairs of areas chosen randomly. The number of shortcuts are determined by the probability ϕ per connection on the underlying ring lattice such that the total shortcuts is $Lk\phi$ on average. By introducing a characteristic length parameter $\xi = 1/(k\phi)$, the average number of shortcuts becomes L/ξ, and the value of ASP can be calculated as [64]

$$ASP = \frac{\xi}{2k\sqrt{1+2\xi/L}} \tanh^{-1} \frac{1}{\sqrt{1+2\xi/L}}.$$

To calculate the entropy of the network, we first describe the spatial location of each area in the ring network by an angular coordinate $2\pi i/L, (i = 1, 2, \ldots, L)$. Subsequently, the distance between the i-th and j-th areas can be calculated as $2\pi|i-j|/L$. To simplify calculation, we assume L is an even number, thus the smallest and largest wiring lengths are $2\pi/L$ and π respectively. We then discretize the wiring length distribution by dividing the distance range into $L/2$ bins evenly, which are $[\frac{3\pi}{2L}, \frac{5\pi}{2L}), [\frac{5\pi}{2L}, \frac{7\pi}{2L}), \ldots, [\pi - \frac{\pi}{2L}, \pi + \frac{\pi}{2L})$. If the probability ϕ for adding a shortcut is zero, there are only L links belonging to each of the first k bins and there is no link in the remaining bins. Whereas if ϕ is nonzero, an average number of $Lk\phi$ shortcuts will

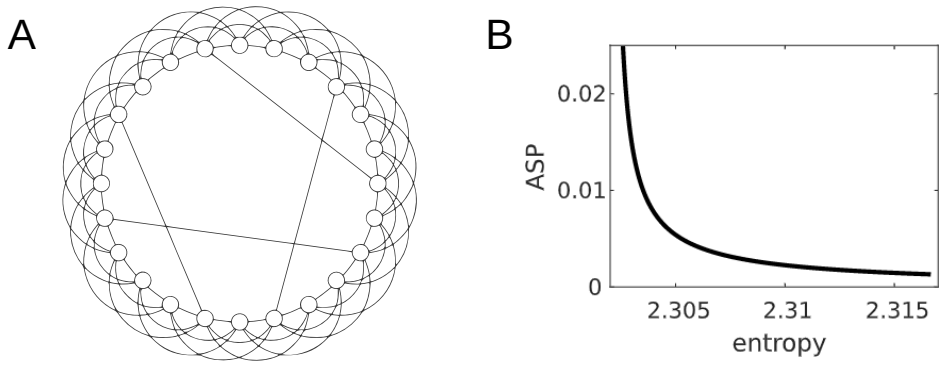

Fig 5. Negative correlation between network entropy and ASP revealed in an idealized brain network. (A) An schematic graph of an idealized brain network with 24 areas and 4 shortcuts. Each area connects to its nearest 6 neighboring areas. (B) ASP negatively correlates with network entropy derived from the mathematical analysis.

be randomly and independently added to the network, hence the lengths of those shortcuts will fall into all the $L/2$ bins with equal probability. On average, each bin will have an identical number of shortcuts as $2k\phi$. And the connection length distribution is approximately

$$P(d \in i\text{th bin}) = \begin{cases} \frac{L}{kL+(L/2-k)2k\phi} & \text{for } i \leq k \\ \frac{2k\phi}{kL+(L/2-k)2k\phi} & \text{for } i > k \end{cases}$$

Correspondingly, we can calculate the entropy as

$$H = -\frac{kL\xi}{kL\xi + L - 2k}\ln(L\xi) - \frac{L-2k}{kL\xi + L - 2k}\ln(2) + \ln(kL\xi + L - 2k).$$

As shown in Fig. 5B, as the parameter ϕ increases, the network entropy increases while the ASP decreases. Therefore, large entropy in this idealized brain network corresponds to small ASP of the network, which supports fast communications between brain areas. Note that by increasing ϕ, the idealized network evolves from regular-lattice network towards small-world network. The latter possesses the features of high clustering coefficient and short ASP, which are similar to those observed in real brain networks.

Therefore, the functional implication of large entropy for supporting efficient communications in the idealized network can remain valid in some brain networks.

To further verify the hypothesis that large entropy or structural diversity correlates with small ASP, we examine the data of real brain networks. For each brain network of the five species, we first construct a corresponding "spatially-regular" network by having each area connecting with a fixed number of spatially nearest neighboring areas. The number of connections is approximately identical for each area and is determined by the way such that the total number of connections in the spatially-regular network is the same as the real brain network. Because most connection lengths are short, the wiring length distribution of this network is narrowly peaked. Accordingly, the network entropy is small. We label the false positive (FP) connections and false negative (FN) connections in the spatially-regular network by comparing it with the real network. We then correct these connections step by step. In each step, we exchange a pair of connections from FP and FN pools which has the shortest length in the pools. Entropy and ASP are calculated throughout the correction steps. After a finite number of steps, the network will be corrected to the real network. As shown in Fig. 6, except for Drosophila and mouse, all the brain networks show the strong negative correlation between network entropy and ASP——the entropy increases while the ASP decreases as the correction continues, indicating that the maximization of network entropy benefits communication efficiency in these networks. For Drosophila and mouse, as the network evolves from spatially-regular to the real one, network entropy increases while ASP remains constant. The insensitivity of ASP for the two networks results from the fact that the networks are densely connected. The ASP thus is small in the presence of a large amount of connections and is independent of network connectivity. Therefore, in these networks, large entropy may have other functional implications, for instance, enhancing functional diversity [32] or robustness [65] of the network, which requires

future investigations.

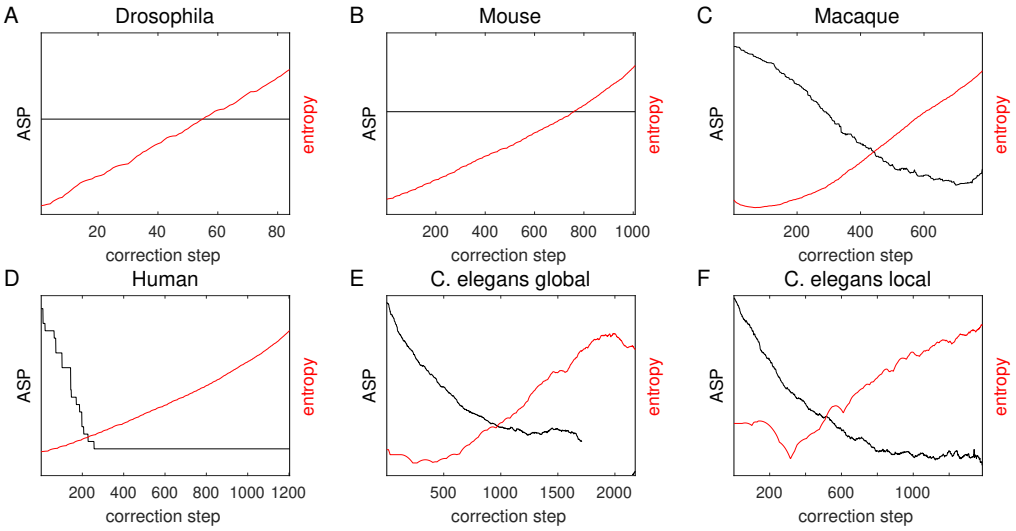

Fig 6. Negative correlation between network entropy and ASP for brain networks of the five species.(A) *Drosophila* network. (B) Mouse network. (C) Macaque network. (D) Human network. (E) Global network of *C. elegans*. (F) Local network of *C. elegans*.

As a network evolves from spatially-regular to the real one by the correction procedure, the material cost of the network also increases. Therefore, the brain network has a larger material cost than the spatially regular network. And in return for this, the brain network has a larger network entropy. This evidence also supports our hypothesis that network structure is optimally formed as a result of the balance between the material cost and structural diversity. Note that the maximization of network entropy shall be a more general principle than the minimization of ASP under the constraint of material cost, as has been hypothesized in previous works [38]. As shown in Fig. 6, the material cost of brain networks for *Drosophila*, Mouse, and Human is able to be further reduced while keeping ASP unchanged. Therefore, these networks do not achieve optimal ASP and material costs.

Discussion

In this work, we have shown that the wiring length distributions of brain networks across multiple species——including *C. elegans*, mouse, macaque, *Drosophila*, and human——share the feature of large entropy. These distributions have been well predicted by maximizing the entropy of wiring length under the constraints of limited wiring material and the spatial locations of neurons or brain areas. In addition, we have proposed a developmental process of random axonal growth to reproduce wiring length distributions for multiple species as measured in experiments, thereby implementing the maximum entropy principle in a biologically plausible manner. We have further developed a generative model incorporating the maximum entropy principle, i.e., the MaxEnt-MinCost model. We have shown that the MaxEnt-MinCost model significantly improves the recovery rate and other network statistics compared with alternative models without accounting for entropy, confirming that entropy maximization involves in determining the structure of brain networks. Our work indicates that the connectivity in brain networks evolves to be structurally diversified to support its complex function such as efficient signal communications between brain areas.

Network functions in general are realized by its dynamics, which can be substantially influenced by network structure [66]. Motivated by this, in this work, we start with network structure *per se* and ask the question of what structural features the brain network optimally evolves to possess under certain spatial and structural constraints. We then discuss the functional implications of the network structure based on our observation of large network entropy across species. This distinguishes our work from previous works attempting to understand network structure from the viewpoint of functional benefits, which lacks a clear definition yet [33, 67–69], .

Although the focus of this work is on brain networks, the maximum entropy principle can be applied to other transport networks beyond brain networks. To demonstrate this,

we have examined networks of Shanghai subway, California Road, and airport in the United States. The data source of these networks can be found in Supplementary Materials. As shown in Fig. S2-S4, under the constraints of limited wiring material and the spatial locations of nodes, the wiring length distributions of these networks can also be well predicted by maximizing the entropy of wiring length. The diversity of network structures is supposed to benefit the efficiency of traffic transport in these networks.

In our work, we have also confirmed that material cost has a crucial impact on network structure [14]. This is demonstrated in the objective function in the MaxEnt-MinCost model $F = H - \lambda\bar{d}$, where H is the network entropy and $\bar{d}$ is the average wiring length. The parameter λ scales the relative importance between the two quantities, and the optimal value of λ that leads to the most accurate network reconstruction is large in general, indicating the importance of the material cost in determine network connectivity. If we view λ as the cost per unit length, as the cost increases, network structure will change accordingly. For instance, as shown in Fig. 7, the networks reconstructed under various λ have distinct clustering coefficients. The larger the λ is, the more expensive the material cost is. As can be inferred from the black curve in Fig. 7, the clustering coefficient has an overall increase under larger material cost with exception at certain λ value. By aligning the best performance λ value shown by the red dashed line, and the experimentally identified network clustering coefficient represented by the red star, we identify that the peaks of clustering coefficient value across species lie around the best "reach" of our generative model. The most distinct peak can be observed in the *C. elegans* local network, implying other unidentified factors recruited in constructing the neural network and leading to even higher clustering coefficient with a moderate material cost. Although the *Drosophila* and mouse networks possess less evidence of this phenomenon, where the recovery rates are already high.

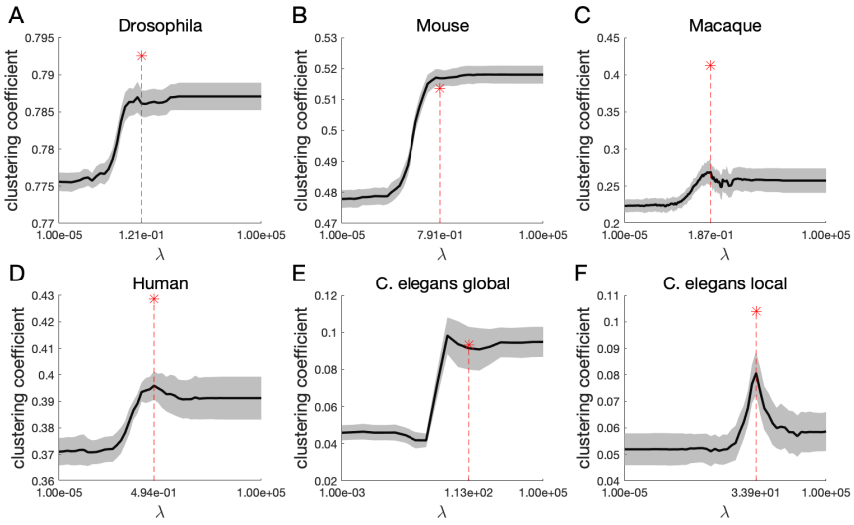

Fig 7.
textbfClustering coefficient varies in the MaxEnt-MinCost network with λ. (A) *Drosophila* network. (B) Mouse network. (C) Macaque network. (D) Human network. (E) Global network of *C. elegans*. (F) Local network of *C. elegans*. The black line is the average clustering coefficient, with shaded grey area as the standard deviation calculated from multiple trials of realization. The red star shows the clustering coefficient value of the corresponding biological brain network. The vertical red dashed line together its value on x-axis give the λ for the best performance MaxEnt-MinCost generative network.

Many algorithms have been proposed for reconstructing neural networks and have achieved good performances [37, 38]. Yet it remains challenging to fully recover the connectivity of a brain network. One challenge lies in the huge space of network configurations. In general, the reconstruction algorithms start with neurons or areas being disconnected. Connections are added gradually based on certain optimization rules. For a network of N nodes, the potential network configurations can be as many as $N!$, which is about $e164$ for the macaque cortical network. Therefore, exhaustive searching is impossible to realize. The MaxEnt-MinCost model partially solves the problem by achieving an accuracy of recovery rate 68% in macaque cortical network, which is comparable with earlier algorithms [37, 38]. Another challenge lies in the identification of factors that determine network structure. The structure of brain networks is determined by various factors, for instance, spatial geometry, gene expression, gradients of growth factors, randomness of axonal growth, and budgets of

energy consumption and material cost. Here we have shown that the network statistics of wiring length distribution is largely determined by the spatial constraint and material cost constraint when maximizing network entropy, and realized by random axonal growth. However, these factors are insufficient to accurately recover network connectivity, as demonstrated by the performance of the MaxEnt-MinCost model. Therefore, to incorporate more factors in the generative model can be a future direction to understand network connectivity. In addition, the MaxEnt-MinCost model can be further modified by taking into account the direction and weight of connections in the future study.

Acknowledgments

References

1. Honey CJ, Kötter R, Breakspear M, Sporns O. Network structure of cerebral cortex shapes functional connectivity on multiple time scales. Proceedings of the National Academy of Sciences. 2007;104(24):10240–10245.
2. Zhou D, Xiao Y, Zhang Y, Xu Z, Cai D. Causal and structural connectivity of pulse-coupled nonlinear networks. Physical review letters. 2013;111(5):054102.
3. Rubino D, Robbins KA, Hatsopoulos NG. Propagating waves mediate information transfer in the motor cortex. Nature neuroscience. 2006;9(12):1549.
4. Muller L, Chavane F, Reynolds J, Sejnowski TJ. Cortical travelling waves: mechanisms and computational principles. Nature Reviews Neuroscience. 2018;19(5):255.
5. Roberts JA, Gollo LL, Abeysuriya RG, Roberts G, Mitchell PB, Woolrich MW, et al. Metastable brain waves. Nature communications. 2019;10(1):1056.
6. Jirsa VK, Haken H. Field theory of electromagnetic brain activity. Physical Review Letters. 1996;77(5):960.
7. Jbabdi S, Sotiropoulos SN, Behrens TE. The topographic connectome. Current opinion in neurobiology. 2013;23(2):207–215.
8. Fornito A, Zalesky A, Breakspear M. The connectomics of brain disorders. Nature Reviews Neuroscience. 2015;16(3):159.
9. Bassett DS, Bullmore E, Verchinski BA, Mattay VS, Weinberger DR, Meyer-Lindenberg A. Hierarchical organization of human cortical networks in health and schizophrenia. Journal of Neuroscience. 2008;28(37):9239–9248.

10. Feinberg I. Schizophrenia: caused by a fault in programmed synaptic elimination during adolescence? Journal of psychiatric research. 1983;17(4):319–334.

11. Bullmore E, Sporns O. Complex brain networks: graph theoretical analysis of structural and functional systems. Nature reviews neuroscience. 2009;10(3):186.

12. Bassett DS, Sporns O. Network neuroscience. Nature neuroscience. 2017;20(3):353.

13. van den Heuvel MP, Kahn RS, Goñi J, Sporns O. High-cost, high-capacity backbone for global brain communication. Proceedings of the National Academy of Sciences. 2012;109(28):11372–11377.

14. Bullmore E, Sporns O. The economy of brain network organization. Nature Reviews Neuroscience. 2012;13(5):336.

15. Meunier D, Lambiotte R, Bullmore ET. Modular and hierarchically modular organization of brain networks. Frontiers in neuroscience. 2010;4:200.

16. Sporns O, Betzel RF. Modular brain networks. Annual review of psychology. 2016;67:613–640.

17. Young MP. Objective analysis of the topological organization of the primate cortical visual system. Nature. 1992;358(6382):152.

18. Hilgetag CC, Burns GA, O'Neill MA, Scannell JW, Young MP. Anatomical connectivity defines the organization of clusters of cortical areas in the macaque and the cat. Philosophical Transactions of the Royal Society of London Series B: Biological Sciences. 2000;355(1393):91–110.

19. Hilgetag CC, Kaiser M. Clustered organization of cortical connectivity. Neuroinformatics. 2004;2(3):353–360.

20. Watts DJ, Strogatz SH. Collective dynamics of 'small-world'networks. nature. 1998;393(6684):440.

21. Bassett DS, Bullmore E. Small-world brain networks. The neuroscientist. 2006;12(6):512–523.

22. He Y, Chen ZJ, Evans AC. Small-world anatomical networks in the human brain revealed by cortical thickness from MRI. Cerebral cortex. 2007;17(10):2407–2419.

23. Barthélemy M. Spatial networks. Springer; 2018.

24. Ramon-y Cajal S, Swanson N, Swanson LW, Guillery R. Histology of the nervous system. Trends in Neurosciences. 1996;19(4):156–156.

25. Stiso J, Bassett DS. Spatial embedding imposes constraints on neuronal network architectures. Trends in cognitive sciences. 2018;.

26. French L, Pavlidis P. Relationships between gene expression and brain wiring in the adult rodent brain. PLoS computational biology. 2011;7(1):e1001049.

27. Rubinov M, Ypma RJ, Watson C, Bullmore ET. Wiring cost and topological participation of the mouse brain connectome. Proceedings of the National Academy of Sciences. 2015;112(32):10032–10037.

28. Chklovskii DB. Exact solution for the optimal neuronal layout problem. Neural computation. 2004;16(10):2067–2078.

29. Hellwig B. A quantitative analysis of the local connectivity between pyramidal neurons in layers 2/3 of the rat visual cortex. Biological cybernetics. 2000;82(2):111–121.

30. Stepanyants A, Hirsch JA, Martinez LM, Kisvárday ZF, Ferecskó AS, Chklovskii DB. Local potential connectivity in cat primary visual cortex. Cerebral Cortex. 2007;18(1):13–28.

31. Kaiser M, Hilgetag CC, Van Ooyen A. A simple rule for axon outgrowth and synaptic competition generates realistic connection lengths and filling fractions. Cerebral Cortex. 2009;19(12):3001–3010.

32. Betzel RF, Bassett DS. Specificity and robustness of long-distance connections in weighted, interareal connectomes. Proceedings of the National Academy of Sciences. 2018;115(21):E4880–E4889.

33. Laughlin SB, Sejnowski TJ. Communication in neuronal networks. Science. 2003;301(5641):1870–1874.

34. Ercsey-Ravasz M, Markov NT, Lamy C, Van Essen DC, Knoblauch K, Toroczkai Z, et al. A predictive network model of cerebral cortical connectivity based on a distance rule. Neuron. 2013;80(1):184–197.

35. Karbowski J. Optimal wiring principle and plateaus in the degree of separation for cortical neurons. Physical review letters. 2001;86(16):3674.

36. Song HF, Kennedy H, Wang XJ. Spatial embedding of structural similarity in the cerebral cortex. Proceedings of the National Academy of Sciences. 2014;111(46):16580–16585.

37. Betzel RF, Avena-Koenigsberger A, Goñi J, He Y, De Reus MA, Griffa A, et al. Generative models of the human connectome. Neuroimage. 2016;124:1054–1064.

38. Chen Y, Wang S, Hilgetag CC, Zhou C. Features of spatial and functional segregation and integration of the primate connectome revealed by trade-off between wiring cost and efficiency. PLoS computational biology. 2017;13(9):e1005776.

39. Cherniak C. Local optimization of neuron arbors. Biological cybernetics. 1992;66(6):503–510.

40. Shannon CE. A mathematical theory of communication. Bell system technical journal. 1948;27(3):379–423.

41. Rubinov M, Sporns O. Weight-conserving characterization of complex functional brain networks. Neuroimage. 2011;56(4):2068–2079.

42. Braitenberg V, Schüz A. Cortex: statistics and geometry of neuronal connectivity. Springer Science & Business Media; 2013.

43. White JG, Southgate E, Thomson JN, Brenner S. The structure of the nervous system of the nematode Caenorhabditis elegans. Philosophical Transactions of the Royal Society of London B, Biological Sciences. 1986;314(1165):1–340. doi:10.1098/rstb.1986.0056.

44. Chen BL, Hall DH, Chklovskii DB. Wiring optimization can relate neuronal structure and function. Proceedings of the National Academy of Sciences. 2006;103(12):4723–4728. doi:10.1073/pnas.0506806103.

45. Chen B. Neuronal Network of C. elegans: from Anatomy to Behavior. Cold Spring Harbor Laboratory; 2007.

46. Varshney LR, Chen BL, Paniagua E, Hall DH, Chklovskii DB. Structural properties of the Caenorhabditis elegans neuronal network. PLoS Computational Biology. 2011;7(2):1–21. doi:10.1371/journal.pcbi.1001066.

47. Achacoso TB YWS. In: Ay's Neuroanatomy of C. Elegans for Computation. CRC Press; 1992. p. 79–164.

48. Durbin RM. Studies On The Development And Organisation Of The Nervous System Of Caenorhabditis Elegans;.

49. Kaiser M, Hilgetag CC. Nonoptimal Component Placement, but Short Processing Paths, due to Long-Distance Projections in Neural Systems. PLOS Computational Biology. 2006;2(7):1–11. doi:10.1371/journal.pcbi.0020095.

50. Choe Y McCormick BH KW. Network connectivity analysis on the temporally augmented C. elegans web: A pilot study. Society of Neuroscience Abstracts. 2004;30(921.9).

51. Kötter R. Online retrieval, processing, and visualization of primate connectivity data from the CoCoMac Database. Neuroinformatics. 2004;2(2):127–144. doi:10.1385/NI:2:2:127.

52. Carmichael ST, Price JL. Architectonic subdivision of the orbital and medial prefrontal cortex in the macaque monkey. Journal of Comparative Neurology. 1994;346(3):366–402. doi:10.1002/cne.903460305.

53. Goldman-Rakic PS, Rakic P. Preface: Cerebral Cortex Has Come of Age. Cerebral Cortex. 1991;1(1):1. doi:10.1093/cercor/1.1.1.

54. Lewis JW, Van Essen DC. Mapping of architectonic subdivisions in the macaque monkey, with emphasis on parieto-occipital cortex. Journal of Comparative Neurology. 2000;428(1):79–111.

55. Chen Y, Wang S, Hilgetag CC, Zhou C. Trade-off between Multiple Constraints Enables Simultaneous Formation of Modules and Hubs in Neural Systems. PLOS Computational Biology. 2013;9(3):1–20. doi:10.1371/journal.pcbi.1002937.

56. Kleitman DJ, Wang DL. Algorithms for constructing graphs and digraphs with given valences and factors. Discrete Mathematics. 1973;6(1):79–88.

57. Grant M, Boyd S. CVX: Matlab Software for Disciplined Convex Programming, version 2.1; 2014. `http://cvxr.com/cvx`.

58. Grant M, Boyd S. Graph implementations for nonsmooth convex programs. In: Blondel V, Boyd S, Kimura H, editors. Recent Advances in Learning and Control. Lecture Notes in Control and Information Sciences. Springer-Verlag Limited; 2008. p. 95–110.

59. Baruch L, Itzkovitz S, Golan-Mashiach M, Shapiro E, Segal E. Using expression profiles of Caenorhabditis elegans neurons to identify genes that mediate synaptic connectivity. PLoS computational biology. 2008;4(7):e1000120.

60. Binzegger T, Douglas RJ, Martin KA. A quantitative map of the circuit of cat primary visual cortex. Journal of Neuroscience. 2004;24(39):8441–8453.

61. Kolmogorov A. Sulla determinazione empirica di una legge di distribuzione. G Ist Ital Attuari. 1933;4:83–91.

62. Smirnov N. Table for Estimating the Goodness of Fit of Empirical Distributions. The Annals of Mathematical Statistics. 1948;19(2):279–281.

63. Newman ME. Modularity and community structure in networks. Proceedings of the national academy of sciences. 2006;103(23):8577–8582.

64. Newman ME, Moore C, Watts DJ. Mean-field solution of the small-world network model. Physical Review Letters. 2000;84(14):3201.

65. Demetrius L, Manke T. Robustness and network evolution—an entropic principle. Physica A: Statistical Mechanics and its Applications. 2005;346(3-4):682–696.

66. Honey CJ, Thivierge JP, Sporns O. Can structure predict function in the human brain? Neuroimage. 2010;52(3):766–776.

67. Antonopoulos CG, Srivastava S, Pinto SEdS, Baptista MS. Do brain networks evolve by maximizing their information flow capacity? PLOS computational biology. 2015;11(8):e1004372.

68. Toker D, Sommer FT. Information integration in large brain networks. PLoS computational biology. 2019;15(2):e1006807.

69. Linsker R. Self-organization in a perceptual network. Computer. 1988;21(3):105–117.